Molecular beam epitaxy of GaSb on vicinal Si(001) substrates: influence of the conditions of layer nucleation on their structural and optical properties

© M.O. Petrushkov[1], M.A. Putyato[1], A.V. Vasev[1], D.S. Abramkin[1,2], E.A. Emelyanov[1], I.D. Loshkarev[1],
O.S. Komkov[3], D.D. Firsov[3], V.V. Preobrazhenskii[1]

[1] Rzhanov Institute of Semiconductor Physics, Siberian Branch, Russian Academy of Sciences,
630090 Novosibirsk, Russia
[2] Novosibirsk State University,
630090 Novosibirsk, Russia
[3] St. Petersburg State Electrotechnical University „LETI",
197022 St. Petersburg, Russia

E-mail: maikdi@isp.nsc.ru

GaSb films were grown by molecular beam epitaxy on vicinal Si(001) substrates with miscut angles of 6° to the (111) plane. Films were formed on AlSb(001)/Al/As/Si, AlSb(00$\bar{1}$)/Al/As/Si, GaSb(00$\bar{1}$)/Ga/P/Si and GaSb(001)/P/Ga/Si transition layers. The influence of orientation, composition, and formation conditions of transition layers on the crystal perfection and optical properties of GaSb films was studied. The GaSb film grown on the GaSb(00$\bar{1}$)/Ga/P/Si(001) transition layer has the best structural and optical properties.

1. Introduction

Structures based on $A^{III}Sb$ are used to create a wide range of IR devices, such as lasers, light-emitting diodes, photodiodes, etc. [1–3]. Recently, the development of technology for producing thin, high-quality GaSb buffer layers on cheap and durable Si substrates has become an urgent task. The use of metamorphic GaSb/Si substrates will significantly reduce the cost of optoelectronic devices based on $A^{III}Sb$ and will provide them with a wide range of applications in special tasks of observation, guidance, protection of objects, control of the composition of the air environment, etc., in which the implementation of limiting device characteristics.

Creating a technology for growing perfect epitaxial layers $A^{III}B^{V}$/Si involves a number of problems. The main ones are: the transition from a non-polar substrate material to a polar film material, the transition from a constant silicon crystal lattice to a constant lattice of the epitaxial layer, a large difference in the coefficients of thermal expansion of the film and substrate materials, as well as the formation of a large number of three-dimensional islands of the compound $A^{III}B^{V}$ at the initial stages of epitaxy on the silicon surface. This leads to the formation of defects in epitaxial films $A^{III}B^{V}$/Si — antiphase domains (APD) and misfit dislocations (MD). The threading branches of the MD and the boundaries of the APD (antiphase boundaries — APB) are extended structural defects that reduce the crystal perfection of the epitaxial layers [4,5]. The search for ways to reduce the density of MD, reduce the area of APB and increase the smoothness of the surface of epitaxial layers $A^{III}B^{V}$/Si is an urgent scientific and applied task, the complexity of which is due to a complex of interrelated fundamental and technological factors.

In 1986 several research groups demonstrated at once [6,7] that single-domain GaAs films can be grown on the surface of Si(001) by the epitaxy method (MBE or MOVPE). A necessary condition for this is the use of substrates deflected by 2−6 angular degrees to the plane (111). Later studies [8–11] have shown that this result is associated with the effect of self-organization of the vicinal surface Si(001) into an ordered array of bilayer steps during annealing under the ultrahigh vacuum conditions (UHVC). Thus, one of the fundamental reasons for the formation of antiphase domains in the system $A^{III}B^{V}$/Si(001) is removed.

Real silicon substrates always have imperfections, such as deviation from the plane, various surface defects, deviation of the direction of miscut from azimuth [110]. Due to these reasons, the process of forming diatomic steps on a real vicinal silicon substrate cannot be brought to full completion. That is, the substrate after the procedure of combining monatomic steps always contains areas with terraces one atomic layer high, on which APD are subsequently formed. In the process of growth of the transition layer to the APD caused by the structure of the substrate, the APD formed as a result of exchange reactions in the system $A^{III}B^{V}$/Si will be added: As/Si [12-18], Sb/Si [19–22], P/Si [23,24].

The direct influence of MD on the morphology of the film is insignificant and is reduced to the formation of system [25], which is an orthogonal grid of steps with a height of several monolayers on the surface (001). If an unordered array of APD is present in the crystal volume in addition to MD, then another mechanism [26] is implemented, which has a significant effect on the formation of the morphology of the growth surface.

The use of a non-polar vicinal substrate for growing polar material allows the formation of films $A^{III}B^V$/Si with different orientations — $A^{III}B^V(001)$/Si(001) and $A^{III}B^V(00\bar{1})$/Si(001) [12]. The singular surfaces (001) and $(00\bar{1})$ of compounds $A^{III}B^V$ cannot be distinguished from the point of view of atomic structure and physico-chemical properties. The differences appear only on vicinal surfaces, on which dimers of group V elements may have different orientations relative to the edges of the terraces. On the vicinal surface $A^{III}B^V(001)$, miscut to the plane (111), the dimers of the elements V groups are parallel to the edges of the terraces, and on the surface $(00\bar{1})$ — are perpendicular.

In the work [27] it was shown that when GaAs grows on vicinal Si substrates, the orientation of arsenic dimers relative to the edges of terraces significantly affects the morphology of the surface of epitaxial films. Thus, another independent factor determining the properties and quality of epitaxial layers $A^{III}B^V$/Si is the orientation of the epitaxial film relative to the vicinal substrate.

In the GaSb/Si heterosystem, the processes of MD grid formation, APD nucleation and islet formation begin already at the deposition of the first monolayers of the compound. In this regard, in the case of the growth of GaSb/Si heterostructures, the composition and conditions of formation of the transition layer between the film and the substrate play a particularly important role. The transition layer can be divided into two sublayers: (1) *conversion layer* (CL), which consists of a bilayer of the type „V−III" or „III−V" and serves as the basis for further epitaxy of compounds $A^{III}B^V$, (2) *is the linking layer*, which is a thin relaxed film. The CL is pseudomorphic with respect to the substrate. The conversion layers can differ both in composition and in the way they are obtained, which sets the orientation of the subsequent layers of compounds $A^{III}B^V$. Simultaneously with the formation of the conversion layer, the APD array is also emerging. The processes of plastic relaxation of the epitaxial layer begin and further develop in close interaction with the changing APD array. It can be expected that the orientation of the vicinal surface of the epitaxial layer will also influence the development of the plastic relaxation process in such a complex system. Thus, in order to create a technology for growing perfect GaSb/Si buffer layers, it is necessary to solve a number of tasks: choosing the orientation of the epitaxial layer relative to the vicinal substrate, choosing the composition and conditions for the formation of conversion and conjugation layers.

In this paper, the influence of orientation, composition and conditions of formation of transition layers between the vicinal Si(001) substrate and the epitaxial GaSb film on its crystal and optical properties is investigated.

2. Experiment

GaSb/Si heterostructures were grown in a molecular beam epitaxy setup „State" (Russia). Crucible sources were used to obtain flows of Ga, Al, Si atoms and Sb_4 molecules, and to obtain flows of As_2 and P_2 molecules— valve sources with a cracking zone [28]. Epitaxy was performed on Si(001) substrates deflected by $6°$ to plane (111). The structural state and morphology of the substrate surface and epitaxial layers were monitored by the reflected high energy electron diffraction (RHEED) method.

The removal of the oxide layer from the Si surface was carried out at the substrate temperature $T_S = 720°C$ in a stream of atomic silicon $6.7 \cdot 10^{12}$ at/cm$^2 \cdot$ c. After removal of the oxide, the substrate was annealed at $T_S = 850°C$ for 30 min under the UHV conditions to form a system of diatomic terraces on the surface Si. When the process of combining the steps was completed, a well-ordered superstructure (2×1) was observed in the RHEED picture. The dimer bonds Si−Si on such a surface are oriented along the edges of the terraces, which is consistent with the data of [12]. After annealing, the substrate was cooled under the UHV conditions to the temperature of the formation of the conversion layer.

In the work [29] it was shown that during the nucleation of GaSb, small islands (~ 20 nm) with high density ($\sim 1.0 \cdot 10^{11}$ cm^{-2} are formed directly on the surface of Si), the coalescence of which forms layers with a high density of defects and a developed surface morphology. In the course of this work, it was also found that growing a GaSb linking layer on conversion layers with different orientations based on arsenic atoms leads to the formation of an insular surface with a developed morphology in the entire range of growth conditions studied by us. The GaSb film disintegrated into islands already during the deposition of the second layer of gallium atoms and was poorly planarized during further growth. In the works [30,31], when growing GaSb on Si(001), AlSb transition layers were used, on which quasi-2D GaSb layers were formed. According to the data of the study [32], the use of AlSb interface layers also significantly improves the quality of GaSb/GaAs layers. Therefore, when forming GaSb films on conversion layers based on arsenic atoms, we used AlSb linking layers. In the works [27,33] it was found that the conversion layer based on As or GaP allows to form a linking layer with the required orientation stably and in a wide range of growth conditions. This result could not be achieved when using a conversion layer based on the bilayers „Sb−Al" and „Al−Sb". In this case, with all the modes of layer formation used by us, GaSb film conversions were obtained with only one orientation (001). Therefore, when using AlSb linking layers, conversion layers based on arsenic atoms were used in the work, which allowed the formation

of GaSb films with orientations (001) and (00$\bar{1}$). In the course of the work, it was found that when using GaP-based conversion layers, quasi-2D GaSb layers are formed without using AlSb interface layers.

When forming CL based on arsenic atoms, depending on the deposition conditions, they are either chemisorbed onto the Si surface without substitution (creating a replica of the substrate surface), or with the substitution of Si atoms in the upper layer [12]. In this case, the As−As bond in dimers turns out to be located either perpendicular or parallel to the edges of the terraces. With the subsequent growth of the compound $A^{III}B^V$, layers with the orientation (00$\bar{1}$) and (001) are formed, respectively. Denote as „As$_{\parallel}$" a layer of arsenic dimers on silicon with dimerization bonds parallel to the edges of the terraces, and „As$_{\perp}$" with bonds perpendicular to the edges of the terraces.

When using from one to several binary GaP layers as a conversion layer, the orientation of the GaP film depends on the sequence of deposition of gallium and phosphorus layers on the surface of the vicinal substrate Si [27]. If a layer of gallium atoms is formed on the substrate surface first, then GaP films with orientation (001) grow in the future (phosphorus dimers are parallel to the edges of the terraces), and if a layer of phosphorus atoms is formed first — GaP(00$\bar{1}$) (phosphorus dimers are perpendicular to the edges terraces) [33].

In the work using arsenic conversion layers, AlSb(001)/Al/As$_{\parallel}$/Si and AlSb(00$\bar{1}$)/Al/As$_{\perp}$/Si linking layers were formed, allowing the growth of GaSb films (001) and GaSb(00$\bar{1}$) respectively. On the basis of the GaP conversion layer, the linking layers GaSb(001)/P$_{\parallel}$/Ga/Si and GaSb(00$\bar{1}$)/Ga/P$_{\perp}$/Si were formed, on which films were grown GaSb(001) and GaSb(00$\bar{1}$) respectively.

The four structures were grown, differing in the conditions of formation and the composition of the transition layers: GaSb(001)/AlSb/As$_{\parallel}$/Si, GaSb(00$\bar{1}$)/AlSb/As$_{\perp}$/Si and GaSb(001)/P$_{\parallel}$/Ga/Si, GaSb(00$\bar{1}$)/Ga/P$_{\perp}$/Si, denoted further in the text as $S_{As_{\parallel}}^{(001)}$, $S_{As_{\perp}}^{(00\bar{1})}$, $S_{P_{\parallel}}^{(001)}$ and $S_{P_{\perp}}^{(00\bar{1})}$ respectively.

The linking layers were formed by the Atomic Layer Epitaxy (ALE). Their thickness was 10 monolayers (ML). The main layers of GaSb with a thickness of 500 nm were grown by the MBE method at a rate of 1 MS/s at $T_S = 400°$C. The relatively low growth temperature was chosen in order to reduce the influence of T_S on the processes of changing the state of the complex of extended and point defects in GaSb films formed at the initial stages of growth. Such an approach made it possible to reveal the influence of the composition and conditions of the formation of transition layers on the properties of epitaxial films, as well as the influence of post-formation annealing on the change of these properties.

The grown structures were divided into two parts. One part was subjected to additional cyclic annealing under the ultrahigh vacuum conditions. The cycle consisted of a heating stage (from 250 to 520°S for 40 s), annealing at a fixed temperature (520°S for 30 s) and natural cooling

(up to 250°C). The five annealing cycles were carried out for each structure.

For comparison, a GaSb/GaSb homoepitaxial structure was grown under similar conditions on a *epi-ready p$^+$-* type substrate. The thickness of the unalloyed epitaxial layer of GaSb was 1 microns.

The morphology of the surface of the films was studied by the Atomic Force Microscopy (AFM). The studies were carried out *ex situ* using a scanning probe microscope Solver P47 in the semi-contact mode. The structural and optical properties of the samples were studied by high-resolution X-ray diffractometry (XRD) and photoluminescence (PL) in the IR range. The diffraction reflection curves were recorded on a two-crystal X-ray diffractometer. The primary beam of the diffractometer was formed by an X-ray tube with a copper anode, a germanium crystal monochromator in the symmetrical reflection position (004) and an output collimator slit with a size of 0.1 mm in the diffraction plane. Since the atomic planes (004) lie at an angle 6° to the surface of the film, two peak widths corresponding to two variants of curve recording are measured on each sample: in the geometry of sliding incidence and sliding reflection. The table shows the average values for two dimensions. Photoluminescence spectra were measured at 10 K on an installation based on the Vertex 80 infrared Fourier spectrometer equipped with a KBr beam splitter and an InSb photodetector cooled with liquid nitrogen [34]. A laser diode with a wavelength of 809 nm was used to excite luminescence. The method described in [35] was used to carry out measurements.

3. Results

3.1. Surface morphology

The AFM images of the surface of the unannealed structures are shown in Fig. 1, *a* and Fig. 2, *a−c*.

The analysis of AFM data revealed the presence of a pronounced anisotropy of the relief on all four samples (see Fig. 1, 2). It can be seen that the main structural elements forming the morphology of the surface are oriented with their more elongated part parallel to the direction [$\bar{1}$10] along the edges of the terraces on the silicon substrate.

Plotting histograms (see Fig. 1, *b*) for each of the studied surfaces allowed us to determine the characteristic vertical size of the relief (parameter H). In addition, the analysis of the parameters of the central peak of the two-dimensional autocorrelation function (2D-ACF) (see Fig. 1, *c*) allowed us to determine the values of the lateral relief dimensions ($L_{[\bar{1}10]}$ and $L_{[110]}$) and the anisotropy parameter ($\chi = L_{[\bar{1}10]}/L_{[110]}$). The quantitative values of the corresponding parameters are shown in Fig. 1, *a*, fig. 2, *a−c* and in the table.

Experimental AFM data, XRD and PL

Sample designation		$S_{As_\perp}^{(00\bar{1})}$	$S_{As_\parallel}^{(001)}$	$S_{P_\perp}^{(00\bar{1})}$	$S_{P_\parallel}^{(001)}$
Orientation of the GaSb film		$(00\bar{1})$	(001)	$(00\bar{1})$	(001)
Composition of the transition layer		AlSb/As$_\perp$	AlSb/As$_\parallel$	GaSb/Ga/P$_\perp$	GaSb/P$_\parallel$/Ga
Vertical relief size, H, nm		2.7	5.6	3.2	5.3
$L_{[\bar{1}10]}$, nm		116.9	84.3	111.9	222.4
$L_{[110]}$, nm		76.3	46.8	61.8	57.1
χ		1.5	1.8	1.8	3.9
FWHM, W, angular sec.	Before annealing	938	1464	1155	957
	After annealing	670	885	630	684
Mechanism of formation of APD systems		Deposition (replication)	Deposition +substitution	Deposition +substitution	Deposition (replication)
Interzonal I_{BE}, rel.units after annealing/before annealing		0.51/0.062	0.04/0.012	2.8/0.045	0.17/0.068

3.2. Structural properties of films GaSb

Based on the analysis of RD data, the values of parameters characterizing the structural perfection of (W — the full width of the peak of the swing curve at its half maximum (FWHM) are obtained) epitaxial layers before and after annealing (see table). The degree of relaxation of all samples was $R > 98\%$.

3.3. Optical properties

The PL spectra of the studied structures measured in the near IR range $(0.74-0.82$ eV) at a temperature of 10 K, are shown in Fig. 3. The black (solid) and red (dashed) lines correspond to the spectra before and after annealing in the UHVC, respectively. Fig. 3, e shows (for comparison) the spectrum of the GaSb/GaSb(001) structure.

The spectrum of homoepitaxial GaSb is characterized by the line BE (interband recombination) at 0.8 eV and the lines A and B (transitions from the conduction band to the acceptor levels [36] at 0.778 and 0.748 eV, respectively). The intensity of the PL peaks of annealed heteroepitaxial structures is 2 orders of magnitude lower than the corresponding peaks of homoepitaxial GaSb. Nevertheless, the main characteristic lines BE and A can be distinguished on the spectra. The lines are shifted to the long-wavelength region in comparison with the peaks of the PL homoepitaxial material. The magnitude of this shift is the same for all annealed structures and amounted to 0.025 eV (as a result, the line B did not fall into the measured range). The splitting of the peaks BE and A is weakly expressed (the line A forms the shoulder of the long-wave wing of the peak BE). As for the spectra of the unannealed structures, the intensity of the PL radiation of these samples is at the level of background values.

4. Discussion

4.1. Crystal structure

Formally, the transition of the film orientation from $A^{III}B^V(001)$ to $A^{III}B^V(00\bar{1})$ when grown on vicinal Si(001) substrates, miscuted to the plane(111), corresponds to a sequential rotation of the film coordinate system around the directions [110] and [001] by 180°. This leads to the fact that the direction [00$\bar{1}$] in the coordinate system of the epitaxial film will coincide with the direction [001] in the coordinate system of the crystal lattice of the substrate, and the direction [110] in the film will coincide with the direction [$\bar{1}$10] substrates. In this case, the dimerization bonds of the atoms of the V group elements forming the surface structure on the faces (001) and (00$\bar{1}$) will be mutually perpendicular.

Due to the significant mismatch of the permanent lattice parameters of the GaSb film and the Si substrate, the MD grid is formed already during the growth of the first few monolayers of the linking layer (GaSb or AlSb). In this case, the density of the MD is determined by the magnitude of this mismatch. The density of the threading branches of the MD during the growth of the film may vary. The magnitude of these changes depends on the thickness of the film, the growth conditions, as well as on the presence of defects in the crystal structure that are not associated with MD. A decrease in the density of threading dislocations both during growth and during subsequent annealing occurs as a result of annihilation of dislocations with different signs. The presence of crystal lattice disturbances at the interface boundary, in the volume of the film and on its surface can change the mobility of dislocations [37]. As a consequence, the presence of such violations will affect the change in the density of threading branches MD. In our case, all GaSb/Si films were grown under the same growth conditions at low temperature (400°C) and had the same thickness. Therefore, the effect of point defects in the volume of all
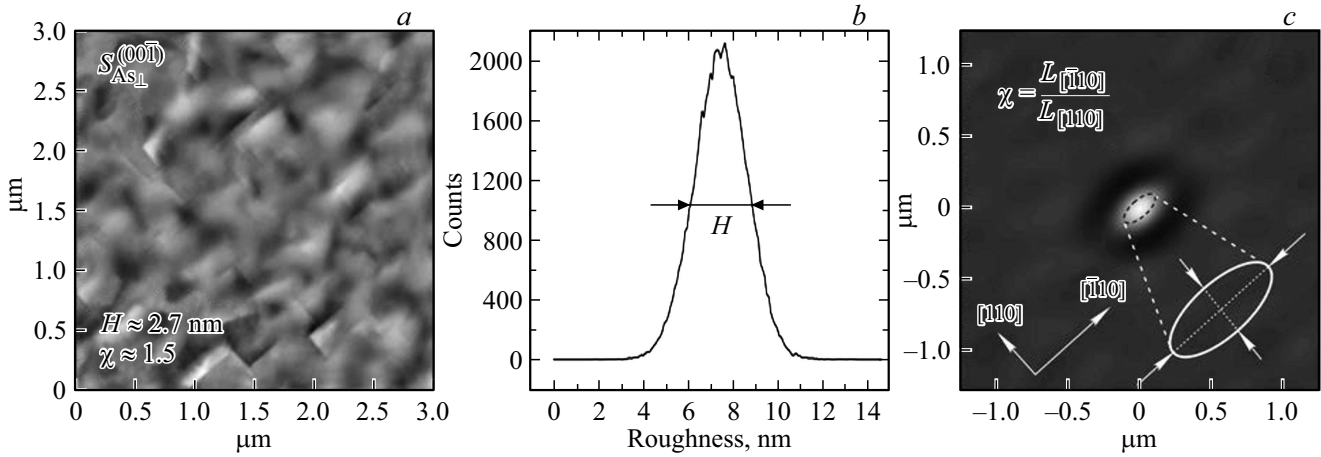
Figure 1. AFM determination of the main relief parameters characterizing the morphology of the sample: a — AFM measurement data for the sample surface $S_{As_\perp}^{(00\bar{1})}$; b — histogram constructed from AFM data (the FWHM of the histogram corresponds to the value of the vertical relief size H), c — analysis of 2D-ACF of AFM data (lateral relief dimensions $L_{[\bar{1}10]}$ and $L_{[110]}$ and the anisotropy parameter χ).
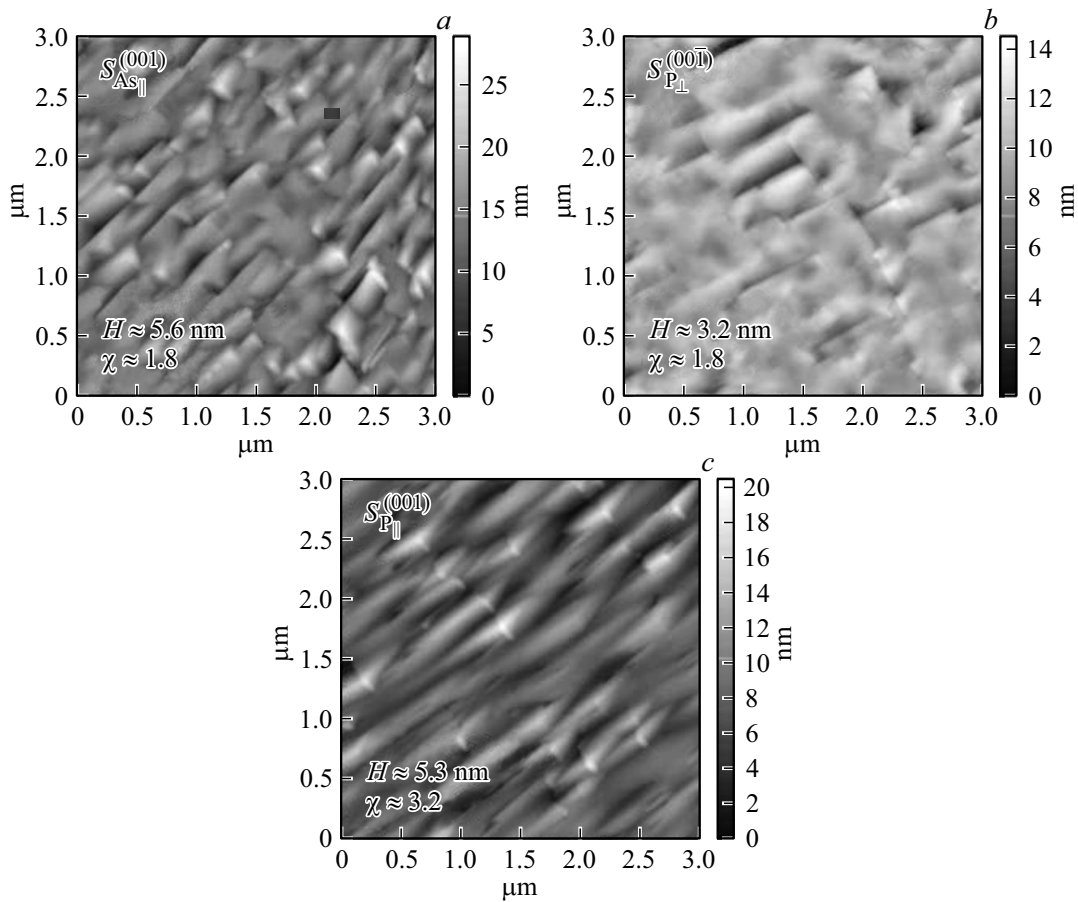
Figure 2. AFM measurement data for sample surfaces: a — $S_{As_\parallel}^{(001)}$, b — $S_{P_\perp}^{(00\bar{1})}$ and c — $S_{P_\parallel}^{(001)}$.
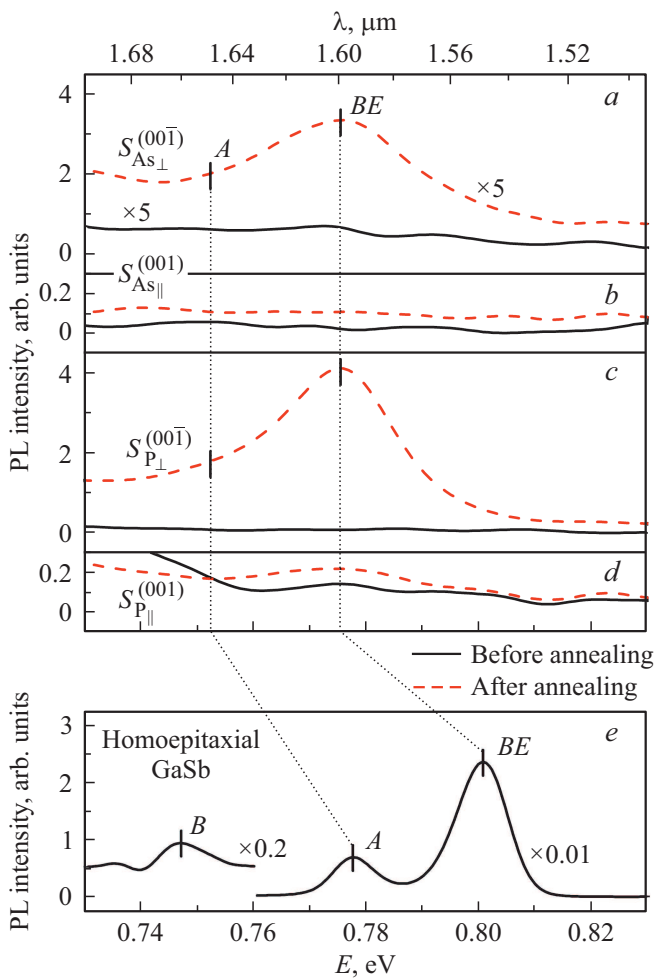
Figure 3. Near-IR PL spectra for structures: a — $S_{As_\perp}^{(00\bar{1})}$, b — $S_{As_\parallel}^{(001)}$, c — $S_{P_\perp}^{(00\bar{1})}$, d — $S_{P_\parallel}^{(001)}$ and e — the homoepitaxial GaSb.

grown films on the movement of the threading branches of the MD will differ slightly. At the same time, the FWHM values of the unannealed samples differ significantly. These differences are due to the influence of extended defects in crystal lattices (not caused by MD). Such defects in our case can be APD.

In this paper, the measurement of the XRD c was carried out to reflect (004). The choice of reflection was due to the fact that the FWHM value of such curves is affected by the density of the MD [38.39], and the presence of an array of APD in the crystal does not affect this characteristic [40,41]. As a result of annealing, the length of the APD boundaries will decrease [41–43] and, as a result, the mobility of the threading branches of the MD will increase. The more the length of the antiphase boundaries decreases during annealing, the more significantly the density of threading dislocations will decrease as a result of their annihilation. These processes should be reflected in the change of FWHM.

From the analysis of the XRD data of the unannealed samples (see table), it follows that the length of the APD

boundaries is higher for $S_{As_\parallel}^{(001)}$ and $S_{P_\perp}^{(00\bar{1})}$ with conversion layers As$_\parallel$ and Ga/P$_\perp$, respectively. Annealing leads to a decrease in FWHM for all samples. This is most clearly manifested for the same samples $S_{As_\parallel}^{(001)}$ and $S_{P_\perp}^{(00\bar{1})}$ (reducing the value of W by 579 and 525 angle.sec, respectively) compared to the samples $S_{As_\perp}^{(00\bar{1})}$ and $S_{P_\parallel}^{(001)}$ (decrease in the value of W by 268 and 273 angle.sec, respectively). It can be assumed that in the case of annealing samples $S_{As_\perp}^{(00\bar{1})}$ and $S_{P_\parallel}^{(001)}$ the decrease in the length of the APD boundaries was smaller than for the samples $S_{As_\parallel}^{(001)}$ and $S_{P_\perp}^{(00\bar{1})}$. This is possible if, before annealing, the distribution of APD by types of their boundaries (type {110} and {111}) it was different for these two pairs of samples. The APDs with inclined walls have the ability to annihilate during annealing [44]. Therefore, in the samples $S_{As_\parallel}^{(001)}$ and $S_{P_\perp}^{(00\bar{1})}$ there were more such domains. Since the initial size distribution of APD for all samples is set by the silicon substrate, the observed difference is unambiguously related to the method of formation of the transition layer.

Let us consider the features of the formation of the conversion layer for samples $S_{As_\perp}^{(00\bar{1})}$, $S_{As_\parallel}^{(001)}$ and $S_{P_\perp}^{(00\bar{1})}$, $S_{P_\parallel}^{(001)}$:

1. The process of forming the conversion layer As$_\perp$/Si for the sample $S_{As_\perp}^{(00\bar{1})}$ occurred at $100 < T_S < 200°$C by chemisorption of arsenic molecules on the surface of silicon atoms without their substitution. At such a low temperature, the implementation of the substitution reaction of silicon atoms with arsenic atoms is practically impossible. A layer of arsenic atoms creates a replica of the substrate surface. At a higher temperature, the substitution process is activated [12]. The structure of the arsenic replica differs from the structure of the reconstructed substrate surface only by the orientation of dimeric bonds relative to the edges of the terraces. Let us recall, that after combining single-layer terraces into two-layer ones, a reconstruction consisting of silicon dimers with a dimerization bond parallel to the edges of the terraces is formed on their surfaces (i.e., parallel to the direction [110]). In some number there are regions with dimers oriented perpendicular to the direction [110]. This is APDs. They are energetically unprofitable, but they persist, for example, due to surface defects or deviation errors from (111). The formation of an arsenic replica does not change the extent and geometry of the boundaries of such areas. Thus, the distribution of APD on the surface remains the same. Only their elemental composition and orientation of the upper layer dimerization bonds change.

The bond of arsenic atoms with silicon atoms is strong (according to our experimental data, noticeable desorption of arsenic from the chemisorbed layer begins at 650°C and higher), therefore, the probability of substitution of arsenic atoms with Al atoms at a low temperature of formation of the AlSb linking layer can be neglected. Therefore, it can be expected that the density and dimensions of the APD in the layers As$_\perp$/Si and Sb/Al/As$_\perp$/Si will be determined mainly by the level of the two-domain silicon substrate.
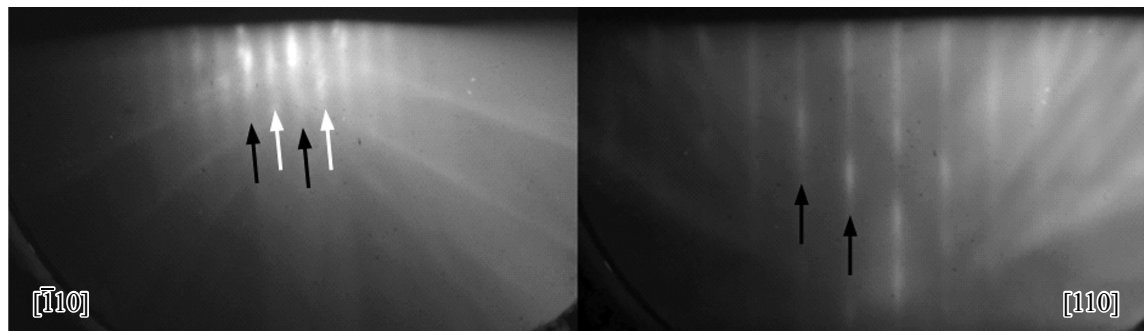
Figure 4. The RHEED pattern from the surface $As_\perp$/Si. The white arrows in the figures indicate fractional reflexes $(0, 1/2)$, the black arrows — basic reflexes.

Fig. 4 shows a picture of the RHEED obtained from the surface $As_\perp$/Si. When observed in azimuth $[\bar{1}10]$ (along the edges of the terraces), fractional reflexes $(0, 1/2)$ are visible. There are no fractional reflexes in azimuth $[110]$, i.e., there is a surface structure (1×2). The basic reflexes show „splitting" caused by diffraction on an ordered system of diatomic terraces. The RHEED pattern allows us to conclude that the $As_\perp$/Si surface is well ordered and that there are a small number of antiphase domains on it. This is consistent with the Scanning Tunneling Microscopy (STM) data from work [12].

2. In the case of the sample $S_{As_\parallel}^{(001)}$, the formation of the conversion layer is also carried out in a stream of arsenic molecules, but at a higher temperature $T_S = 450°C$. The consequence of an increase in the substrate temperature is a change in the chemisorption mechanism from deposition to substitution (arsenic replaces silicon atoms in the upper layer [12]). The orientation of chemisorbed arsenic dimers repeats the orientation of silicon dimers substituted by them. Substitution occurs both at the edges and on the surface of the terraces. In this case, no solid substitution layer is formed [45].

The process of forming a continuous replacement layer with replication of the initial antiphase relief of the substrate surface is complicated by a number of reasons. In the first, APDs on two-layer vicinal terraces Si are energetically unprofitable. It is likely that single-layer terraces with an antiphase dimer structure will be supplemented with arsenic atoms by the chemisorption mechanism without substitution of Si. Within their limits, the structure of As dimers is formed with the orientation of dimerization bonds as in the main phase. In this case, the initial antiphase anomalies in the silicon terrace system will be compensated by arsenic atoms. Secondly, there is some probability of the formation of regions on the surface with the main phase, on which the „replica" is initially formed, preventing the further process of substitution [46]. Thus, new antiphase regions appear on the basis of layers of atoms As. Thirdly, the replacement process is facilitated by mechanical stresses of the reconstructed surface Si. When the compensation of mechanical stresses due to changes in the composition

of the upper layer of the terrace atoms reaches a certain level, the substitution process slows down, as it becomes energetically unprofitable [45]. Presumably, the areas of the terrace surface on which substitution could not be realized are engaged in arsenic dimers by the deposition mechanism. During the formation of the Al layer by the ALE method, a cationic sublayer of AlSb(001) domains is formed on the substituted areas of the terrace surface, and on unsubstituted — AlSb(00$\bar{1}$). As a result, a complex consisting of several subsystems of the AlSb APD with a general predominance of the AlSb(001) phase is formed, which differs in its architecture from the structure of the original APD system on the surface of the silicon substrate.

Fig. 5 shows a picture of the RHEED from the surface of $As_\parallel$/Si obtained during the deposition of arsenic by the substitution mechanism at 450°C. In the azimuth $[\bar{1}10]$, shortened fractional reflexes $(0, 1/2)$ are observed. In the azimuth $[110]$ fractional reflexes $(0, 1/2)$ are narrower and longer. Thus, a mixed reconstruction (2×2) of the surface is observed in the RHEED picture, on which both types of domains $As_\perp$/Si and $As_\parallel$/Si are represented. Clearer fractional reflexes $(0, 1/2)$ in azimuth $[110]$ indicate that the $As_\parallel$/Si phase prevails. The result obtained is consistent with the data of the work [12].

3. Let us consider the CL formation for the sample $S_{P_\perp}^{(00\bar{1})}$. The chemisorption process was carried out at $T_S = 400-500°C$. According to our data, the lower temperature makes it difficult for phosphorus atoms to interact with the surface of Si. Fig. 6 shows the pictures of the RHEED from the Si surface terminated with phosphorus, obtained in azimuths $[\bar{1}10]$ and $[110]$. Well-ordered structures with fractional reflexes $(0, 1/2)$ are observed in both azimuths, which indicates the two-domain nature of the surface. Presumably, the layer $P_\perp$/Si when the sample grows $S_{P_\perp}^{(00\bar{1})}$ was formed by a mixed mechanism both by simple chemisorption and by substitution of Si, similar to the CL in $S_{As_\parallel}^{(001)}$. The substitution of silicon atoms by phosphorus atoms can also be limited by mechanical stresses [23,24,47]. In this case, a mosaic system is formed consisting of domains of P atoms that have replaced Si atoms, and domains consisting of the remaining unsubstituted silicon atoms. At the CL formation
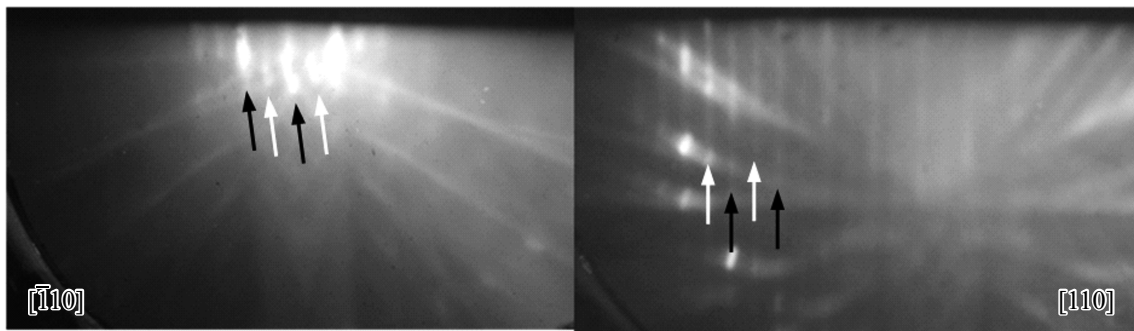
Figure 5. The RHEED pattern from the surface $As_{\parallel}$/Si. The white arrows in the figures indicate fractional reflexes $(0, 1/2)$, the black arrows — basic reflexes.
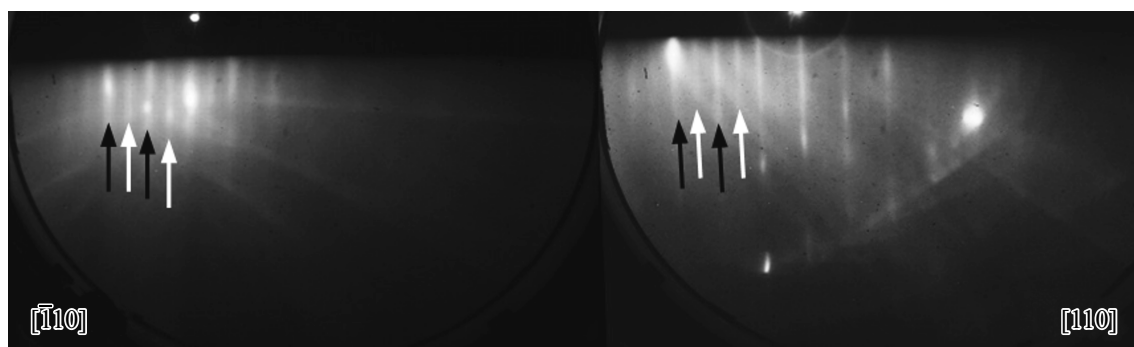
Figure 6. The RHEED pattern from the surface $P_{\perp}$/Si. The white arrows in the figures indicate fractional reflexes $(0, 1/2)$, the black arrows — basic reflexes.

temperature, unsubstituted silicon atoms are subsequently closed by phosphorus dimers.

A layer of gallium atoms on the phosphorus-terminated silicon surface was formed by the ALE method. At the same time, gallium atoms are able to replace phosphorus atoms. Presumably, Ga atoms enter into an exchange reaction with phosphorus atoms that have been chemisorbed without replacing silicon atoms. This is an activation process, and at $T_S > 400°C$, it begins to significantly affect the composition of the conversion layer based on phosphorus atoms. At $T_S > 450°C$, gallium atoms almost completely replace phosphorus atoms [33]. In order to suppress the substitution process, the formation of the Ga layer on $P_{\perp}$/Si was carried out at $T_S = 330°C$. But even at this temperature, there remains some probability of exchange reactions. Therefore, they must be taken into account when considering the process of the nucleation of the first GaP/Si layer. As a result of the substitution of phosphorus atoms with gallium atoms in a certain amount, sites with cationic sublayers are formed on which GaSb(001) domains will grow. Gallium atoms, which are chemisorbed on deposited phosphorus atoms without their substitution, form the domains GaP($00\bar{1}$) — the basis of domains GaSb($00\bar{1}$). With $T_S = 330°C$, this is the dominant process. With phosphorus atoms replacing silicon atoms, Ga atoms do not enter into exchange reactions, but form GaP(001)

domains on them. As a result of the described processes, a two-domain system is formed, consisting of relatively small domains with different phases and differing from the original antiphase system on the surface of the silicon substrate.

4. The conversion layer $P_{\parallel}$/Ga/Si with the growth of the sample $S_{P_{\parallel}}^{(001)}$ was formed by simple chemisorption of gallium atoms on the silicon surface at $T_S = 330°C$. After the deposition of a layer of Ga atoms, a surface structure with the symmetry of the volume lattice (1×1) is observed. The subsequent layer of phosphorus atoms was deposited at the same T_S. Under these conditions, phosphorus atoms are not able to replace gallium atoms and form a layer $P_{\parallel}$/Ga/Si also with reconstruction (1×1). Therefore, the formation of APD nucleus in the case of the formation of a $P_{\parallel}$/Ga/Si interface layer can be neglected and only antiphase regions due to the initial structure of the silicon substrate surface can be considered. The formation of the Ga/Si linking layer is close to the situation with the $As_{\perp}$/Si linking layer discussed above. Valid films $S_{As_{\perp}}^{(00\bar{1})}$ and $S_{P_{\parallel}}^{(001)}$, grown using these conjugation layers, have close values of FWHM — 938 and 957 angle.sec, respectively (see table).

Now let's consider the effect of annealing on the studied samples. In work [48] it was shown that on the areas of the surface $P_{\perp}$/Si with a substitution APD structure (which have a small size and a „well" monolayer depth in base), APDs with inclined boundaries are formed, which are easier to

annihilate and dissolve (dissolution) during annealing. Thus, during the films annealing process, the volume of APD decreases. As a result, a decrease in the length of the APB facilitates the process of dislocation sliding, which leads to a final decrease in the density of the MD threading branches. This process is reflected in a significant reduction in the FWHM of the annealed sample $S_{P_\perp}^{(00\bar{1})}$. This effect, along with the fact of a more effective decrease in the value of FWHM per unit of annealing time (almost by 2 times), can only be explained by a large number of additionally formed small-sized APDs during the formation of the transition layer.

Annealing of the film $S_{As_\parallel}^{(001)}$ also led to a significant decrease in the FWHM value (see table), but its final value turned out to be the largest among all samples. This can be explained by the lower efficiency of the „process of splitting into parts " large-sized APDs (domains whose origin was determined by the initial structure of the substrate) by those substitution domains that are subsequently formed during arsenic deposition. In addition, the formation of the AlSb interface layer can significantly reduce the rate of APB promotion and, as a result, the process of smoothing APB (the Al−Sb bond is stronger than the Ga−Sb bond). Both of these moments may be the reason for a higher FWHM value (885 angle.sec) after annealing for $S_{As_\parallel}^{(001)}$.

Samples have $S_{P_\parallel}^{(001)}$ and $S_{As_\perp}^{(00\bar{1})}$ as a result of annealing, there were similar decreases in FWHM (see table), and they reached similar values (684 and 670 angles.sec, respectively). This is explained by the similar characteristics (number, size and shape) of APD arrays formed on homogeneous CL under conditions suppressing exchange reactions (APD arrays are given by a silicon substrate).

4.2. Surface morphology

Analysis of the AFM data showed that the orientation of the anisotropy of the relief of all the studied films correlates with the orientation of the steps on the surface of the silicon substrate (the relief elements are most elongated in the direction along the edges of the steps). This orientation is not affected by the composition and method of formation of the transition layer, which determine the orientation of the dimers of the V group atoms relative to the edges of the terraces.

The vertical relief size of the films H depends on their orientation. The table shows that for films with orientation $(00\bar{1})$ H. The parameter has approximately 2 times smaller value than for films with orientation (001). The films $GaSb(00\bar{1})$ (samples $S_{As_\perp}^{(00\bar{1})}$ and $S_{P_\perp}^{(00\bar{1})}$) are characterized by close values of the parameters $L_{[\bar{1}10]}$ and $L_{[110]}$, regardless of the composition of the conversion layer. On the contrary, for the films $GaSb(001)$ the composition of the conversion layer affects the value of the parameter $L_{[\bar{1}10]}$. The film $GaSb(001)$ (sample $S_{As_\parallel}^{(001)}$) the value of the parameter $L_{[\bar{1}10]}$ for the conversion layer $As_\parallel$ is 2.6 times

smaller than the corresponding parameter for the conversion layer $P_\parallel$ (sample $S_{P_\parallel}^{(001)}$). At the same time, the relief size in the direction [110] does not depend on the composition of the conversion layer for these samples.

Thus, the orientation of the film affects the terrain parameters. The influence on the relief of the composition and method of formation of the transition layer is manifested in the case of orientation (001) and is expressed in a change only in the lateral size of $L_{[\bar{1}10]}$. The direction of dimeric bonds relative to the edges of the terraces determines the characteristics of the anisotropy of embedding and diffusion of adatoms over the surface. In our case, changing the orientation of dimers does not lead to a change in the orientation of the relief. Therefore, we can assume the existence of a more powerful factor than the anisotropy of embedding and diffusion, which determines the orientation of the anisotropy of the relief. Such a factor may be the structural features formed along the substrate steps at the initial stages of the nucleation of GaSb films during the deposition of conversion and linking layer, when the formation of a grid of MD and arrays of APD occurs. The mechanisms of the influence of threading dislocations on the morphology [25,26] do not allow the formation of a relief with the observed dimensions. Therefore, the most probable reason for the formation of relief anisotropy remains the presence of an APD array, which nucleate mainly at the edges of terraces during the formation of the conversion layer [12].

In the samples $S_{As_\perp}^{(00\bar{1})}$ and $S_{P_\parallel}^{(001)}$, in which the conversion layer is formed by the replica mechanism (which preserves the domain structure of the substrate), the characteristics of the APD arrays differ slightly. At the same time, the relief of the sample surface is $S_{As_\perp}^{(00\bar{1})}$ is smaller anisotropic and has a smaller vertical size. Consequently, the relief parameters in this case are influenced by the anisotropy of diffusion and embedding of adatoms.

On the reconstructed $GaSb(001)$ face, the direction of the greatest diffusion coefficient of gallium adatoms coincides with the direction of the steps. At the same time, in their movement in the direction of [110], gallium adatoms encounter regular obstacles in the form of vicinal steps. Difficulties with overcoming the steps are caused by the Schwebel barriers [49]. This combination of these factors enhances the anisotropy of diffusion and, as a consequence, the anisotropy of the relief. In the case of $GaSb(00\bar{1})/Si$, the direction of the greatest diffusion coefficient of gallium adatoms is perpendicular to the edges of the terraces. At the same time, the presence of Schwebel barriers leads to a decrease in the difference between the effective diffusion coefficients in both directions and, consequently, to a decrease in the anisotropy of the relief.

As discussed in sec. 4.1, y samples $S_{As_\parallel}^{(001)}$ and $S_{P_\perp}^{(00\bar{1})}$ the formation of the conversion layer led to the emergence of a complex APD system, different from the original one formed on the surface of the silicon substrate in the

process of combining single-layer terraces into two-layer ones. The morphology, size, density, and distribution pattern of the newly formed domains depended on the conditions of deposition of the conversion and linking layers, which resulted in a difference in the relief parameters of these samples. Thus, the difference in the morphology of the grown samples is explained by their orientation and the presence of different arrays of APD in them.

4.3. Photoluminescence

In the studied structures, GaSb layers are grown at the same values of substrate temperature, growth rate and ratio of fluxes of gallium atoms and antimony molecules and have equal thicknesses. This makes it possible to compare the properties of films depending on their crystallographic orientation, set by the conversion layer, and the method of formation of this layer. The structure of the APD system is determined by the composition and mechanism of CL formation, and the orientation of the film sets the direction of the dimerization bonds of the V group atoms relative to the edges of the vicinal terraces. Presumably, the combined action of these factors influences the formation and joint evolution of a complex of extended and point defects both during the nucleation, plastic relaxation and growth of GaSb films, and during their annealing, which should be reflected in the spectra PL.

Quantitative analysis of the photoluminescence data of GaSb layers is difficult due to the low intensity of the peaks of interband recombination (I_{BE}), especially in unannealed samples. The following is a qualitative comparison of photoluminescence data of annealed samples. The comparison was carried out under the simplifying assumption that the intensity of the interband PL is inversely proportional to the probability of recombination without radiation at a wavelength BE, which in turn is associated with the concentration of centers of non-radiative and radiative recombination on defects.

The intensity of PL increases in the series $S_{As_\parallel}^{(001)}$, $S_{P_\parallel}^{(001)}$, $S_{As_\perp}^{(00\bar{1})}$, $S_{P_\perp}^{(00\bar{1})}$ as 0.04, 0.17, 0.51 and 2.8 rel.units respectively. The PL intensities of structures with the same orientation in the case of CL based on phosphorus layers have a higher value compared to samples with a conversion layer based on arsenic atoms. But it is difficult to draw any conclusions from this sequence. Further, samples grown with different combinations of factors affecting the properties of structures are compared. So, in the case $S_{P_\perp}^{(00\bar{1})}$ and $S_{As_\perp}^{(00\bar{1})}$ there is an increase in intensity in ~ 5.5, and in the case $S_{P_\parallel}^{(001)}$ and $S_{As_\parallel}^{(001)}$ — in ~ 4.3. In these pairs, the samples differ in the method of CL formation and its composition. The following data are given under the combined influence of the orientation of the film and the formation mechanism for different compositions of CL. It turns out that the radiation intensity of the sample is $S_{P_\perp}^{(00\bar{1})}$ above radiation $S_{P_\parallel}^{(001)}$ in ~ 16.5 times, and in the case of $S_{As_\perp}^{(00\bar{1})}$ and $S_{As_\parallel}^{(001)}$

this parameter equals ~ 12.8. It is noteworthy that in the case of CL formed by replication, the intensity of $S_{As_\perp}^{(00\bar{1})}$ in relation to $S_{P_\parallel}^{(001)}$ the most by 3 times. A with a mixed mechanism of CL formation, the intensity of PL $S_{P_\perp}^{(00\bar{1})}$ higher intensity $S_{As_\parallel}^{(001)}$ by 70 times. Possible reasons for the observed behavior of I_{BE} depending on the orientation of the films, the method of formation of the CL and its composition are discussed further.

The pairwise comparison of intensities presented above confirms that three factors play a leading role in variations in the optical properties of samples: 1) orientation of the GaSb film; 2) method of CL formation; 3) the CL composition. At the same time, the last two factors are interrelated.

The influence of the orientation of the GaSb epitaxial film on I_{BE} is due to the fact that with the two-dimensional layer growth of the compound $A^{III}B^V$ on the vicinal surface (001) the kinetics of embedding impurities and the formation of intrinsic point defects it is sensitive to the orientation of dimerization bonds relative to the direction [110] [50]. The level of influence of orientation allows us to estimate the intensity of the PL films of GaSb samples $S_{As_\perp}^{(00\bar{1})}$ and $S_{P_\parallel}^{(001)}$, since both samples were grown on replicas repeating the original antiphase system of silicon substrates. Thus, the influence of the CL formation mechanism and its composition is minimized. Comparison of the radiation intensity of pairs of samples $S_{P_\perp}^{(00\bar{1})}$, $S_{P_\parallel}^{(001)}$ and $S_{As_\perp}^{(00\bar{1})}$, $S_{As_\parallel}^{(001)}$ also indirectly confirms the influence of the orientation of the GaSb film on I_{BE}.

The conversion layers obtained by the mixed mechanism significantly change the PL properties of GaSb films. At the same time, the role of the composition becomes dominant. The conversion layer formed on the basis of arsenic atoms reduces the intensity of PL in relation to replicas, and the use of phosphorus atoms — increases it many times. The reasons are probably as follows. The structures contain MD, point defects and APD. They all have a different nature. The concentration of MD is set by the mismatch of the constant lattice of the GaSb film and the substrate Si. The structure of the APD system is determined by the method of forming CL. The concentration of point defects is determined by the growth parameters and the direction of deviation of the film from the singular face (001). Moreover, the listed systems of structural defects are able to interact with each other.

It is known that APDs are able to wedge out during film growth, and annealing of [51,52] contributes to a decrease in their size and concentration. Therefore, the bulk of the GaSb film in annealed samples is probably free of APD [53]. However, the presence of the APD system at the stage of plastic relaxation of the epitaxial layer and during its further growth, up to the moment of their wedging, determines the nature of the distribution of threading dislocations in the volume of the GaSb film. Annealing reduces the concentration of threading dislocations and point defects,

but it is difficult to completely get rid of them. The interaction of a system of threading dislocations, APD and an ensemble of point defects during annealing affects the spatial distribution of the latter in the volume of the film GaSb.

Due to the different chemical activity and sizes of arsenic and phosphorus atoms, antiphase systems based on them differ. This is especially pronounced with a mixed mechanism, when the APD system of the Si substrate is replaced by a system based on V group atoms with the involvement of the upper layer of silicon atoms in the process. Probably, in the case of phosphorus atoms, APDs are formed in GaSb, which are earlier wedged out during growth and exhibit greater sensitivity to annealing. Antiphase domains, when using As-based CL, grow deeper into the film and are more stable during annealing, which prevents a more effective reduction in the density of threading dislocations. Presumably, I_{BE} is determined precisely by the complexes of point defects and threading dislocation branches formed during annealing, which is of interest for further research.

5. Conclusion

The influence of orientation, composition and conditions of formation of transition layers between a silicon substrate and an epitaxial GaSb film on its structural and optical properties has been studied. The substrates Si(001) were used, miscuted by $6°$ to the plane (111). GaSb films were grown by molecular beam epitaxy on transition layers AlSb(001)/Al/As$_\parallel$/Si, AlSb(00$\bar{1}$)/Al/As$_\perp$/Si, GaSb(00$\bar{1}$)/Ga/P$_\perp$/Si and GaSb(001)/P$_\parallel$/Ga/Si formed by atomic layer epitaxy. The properties of GaSb films were largely determined by the method of forming the first bilayer of the compound A^{III}B^V (conversion layer).

The elemental composition and the mechanism of formation of the conversion layer determine the crystallographic orientation and structure of the system of antiphase domains of epitaxial layers growing on it. The mechanisms of formation of the conversion layer, in which the first layer consists of atoms of elements of the V group, differ in the ability of these atoms to replace silicon atoms under selected conditions. If there is no substitution, then a replica of the silicon substrate surface is formed while preserving the distribution, extent, and geometry of the boundaries of the original system of antiphase domains of the substrate. In the presence of substitution reactions, a new system of antiphase domains with a different distribution, extent and geometry of boundaries is formed. Depending on the conditions, arsenic atoms can form the first layer both by the substitution mechanism and by the mixed mechanism. Under the selected conditions, based on phosphorus atoms, the first layer can be formed only by a mixed mechanism, and gallium atoms form only a replica. The structure of the formed system of antiphase domains determines the efficiency of their wedging during growth and their sensitivity to annealing.

The observed structural properties of GaSb films are presumably a consequence of the interaction of antiphase domain systems and mismatch dislocations during the growth of the GaSb film and post-annealing of the finished structure. The optical properties of GaSb films are determined by the existing complex of point defects and a system of threading dislocations. It is shown that the orientation of the film affects the concentration of defects that reduce the intensity of radiation of interband recombination in it. The lowest concentration of defects was obtained in GaSb layers (00$\bar{1}$). Presumably, this is due to the orientation of the bonds of atoms III and V groups relative to the edges of the terraces during the formation of GaSb films. The improvement of the structural and optical properties of the samples is observed in the row: $S_{As_\parallel}^{(001)}$, $S_{P_\parallel}^{(001)}$, $S_{As_\perp}^{(00\bar{1})}$, $S_{P_\perp}^{(00\bar{1})}$.

Conflict of interest

The authors declare that they have no conflict of interest.

References

[1] A. Joullie, P. Christol. Comptes Rendus Physique, **4** (6), 621 (2003).
[2] M. Razeghi, A. Haddadi, A.M. Hoang, E.K. Huang, G. Chen, S. Bogdanov, S.R. Darvish, F. Callewaert, R. McClintock. Infr. Phys. Technol., **59**, 41 (2013).
[3] A. Nainani, T. Irisawa, Z. Yuan, B.R. Bennett, J. Brad Boos, Y. Nishi, K.C. Saraswat. IEEE Trans. Electron Dev., **58**, 3407 (2011).
[4] G. Brammertz, Y. Mols, S. Degroote, V. Motsnyi, M. Leys, G. Borghs, M. Caymax. J. Appl. Phys., **99** (9), 093514 (2006).
[5] K. Mukherjee, C.H. Reilly, P.G. Callahan, G.G.E. Seward. J. Appl. Phys., **123** (16), 165701 (2018).
[6] M. Kawabe, T. Ueda. Jpn. J. Appl. Phys., **25** (4), L285 (1986).
[7] T. Ueda, S. Nishi, Y. Kawarada, M. Akiyama, K. Kaminishi. Jpn. J. Appl. Phys., **25** (9), L789 (1986).
[8] D.E. Aspnes, J. Ihm. Phys. Rev. Lett., **57** (24), 3054 (1986).
[9] T. Sakamoto, G. Hashiguchi. Jpn. J. Appl. Phys., **25** (1) L78(1986).
[10] D.J. Chadi. Phys. Rev. Lett., **59** (15), 1691 (1987).
[11] T. Nakayama, Y. Tanishiro, K. Takayanagi. Jpn. J. Appl. Phys., **26** (4), L280 (1987).
[12] R.D. Bringans, D.K. Biegelsen, L.E. Swartz. Phys. Rev. B, **44** (7), 3054 (1991).
[13] P.R. Pukite, P.I. Cohen. Appl. Phys. Lett., **50** (24), 1739 (1987).
[14] R.S. Becker, T. Kutsner, J.S. Vicker. J. Microsc., **152** (1), 157 (1988).

[15] T. Ide. Phys. Rev. B, **51** (3), 1722 (1995).

[16] M.D. Jackson, F.M. Leibsle, R.J. Cole, D.A.C. Gregory, D.A. Woolf, P. Weightman. J. Vac. Sci. Technol. B, **14** (4), 2424 (1996).

[17] T.R. Ohno, E.D. Williams. J. Vac. Sci. Technol. B, **8** (4), 874 (1990).

[18] J. Gryko, R.E. Allen. MRS Online Proceedings Library (OPL), **280**, 65 (1993).

[19] J. Nogami, A.A. Baski, C.F. Quate. Appl. Phys. Lett., **58** (5), 475 (1991).

[20] Y.W. Mo. Phys. Rev. B, **48** (23), 17233 (1993).

[21] H.B. Elswijk, E.J. van Loenen. Ultramicroscopy, **42**, 884 (1992).

[22] B. Garni, I.I. Kravchenko, C.T. Salling. Surf. Sci., **423** (1), 43 (1999).

[23] P. Sen, B.C. Gupta, I.P. Batra. Phys. Rev. B, **73** (8), 085319 (2006).

[24] Y. Wang, X. Chen, R.J. Hamers. Phys. Rev. B, **50** (7), 4534 (1994).

[25] J.W. Matthews, A.E. Blakeslee. J. Cryst. Growth, **27**, 118 (1974).

[26] M. Niehle, J.B. Rodriguez, L. Cerutti, E. Tournié, A. Trampert. Phys. Status Solidi (RRL), **13** (10), 1900290 (2019).

[27] E.A. Emelyanov, D.F. Feklin, M.A. Putyato, B.R. Semyagin, A.K. Gutakovsky, V.A. Seleznev, A.P. Vasilenko, D.S. Abramkin, O.P. Pchelyakov, V.V. Preobrazhensky, N. Zhicuan, N. Haiqiao. Avtometriya, **50** (3), 13 (2014). (in Russian).

[28] M.A. Putyato, V.V. Preobrazhenskii, B.R. Semyagin, D.F. Fëklin, N.A. Pakhanov, E.A. Emelianov, S.I. Chikichev. Semicond. Sci. Technol., **24** (5), 055014 (2009).

[29] R. Machida, R. Toda, S. Fujikawa, S. Hara, I. Watanabe, H.I. Fujishiro. Phys. Status Solidi B, **253** (4), 648 (2016).

[30] K. Akahane, N. Yamamoto, S. Gozu, A. Ueta, N. Ohtani. J. Cryst. Growth, **283** (3–4), 297 (2005).

[31] S.H. Vajargah, S. Ghanad-Tavakoli, J.S. Preston, R.N. Kleiman, G.A. Botton. J. Appl. Phys., **114** (11), 113101 (2013).

[32] H.S. Kim, Y.K. Noh, M.D. Kim, Y.J. Kwon, J.E. Oh, Y.H. Kim, J.Y. Lee, S.G. Kim, K.S. Chung. J. Cryst. Growth, **301**, 230 (2007).

[33] M.A. Putyato, B.R. Semyagin, E.A. Emelyanov, D.F. Feklin, A.P. Vasilenko, V.V. Preobrazhensky. Izv. vuzov. Fizika, **53** (9/2), 293 (2010). (in Russian).

[34] A.I. Luferau, D.D. Firsov, O.S. Komkov. J. Phys.: Conf. Ser., **1400** (6), 066035 (2019).

[35] D.D. Firsov, O.S. Komkov, V.A. Solov'ev, P.S. Kop'ev, S.V. Ivanov. J. Phys. D: Appl. Phys., **49** (28), 285108 (2016).

[36] W. Jakowetz, W. Rühle, K. Breuninger, M. Pilkuhn. Phys. Status Solidi A, **12** (1), 169 (1972).

[37] A. Georgakilas, J. Stoemenos, K. Tsagaraki, P. Komninou, N. Flevaris, P. Panayotatos, A. Christou. J. Mater. Res., **8** (8), 1908 (1993).

[38] P. Gay, P.B. Hirsch, A. Kelly. Acta Metallurgica, **1** (3), 315 (1953).

[39] V.M. Kaganer, O. Brandt, A. Trampert, K.H. Ploog. Phys. Rev. B, **72** (4), 045423 (2005).

[40] A. Létoublon, W. Guo, C. Cornet, A. Boulle, M. Veron, A. Bondi, O. Durand, T. Rohel, O. Dehaese, N. Chevalier, N. Bertru, A. Le Corre. J. Cryst. Growth, **323** (1), 409 (2011).

[41] W. Guo, A. Bondi, C. Cornet, A. Létoublon, O. Durand, T. Rohel, S. Boyer-Richard, N. Bertru, S. Loualiche, J. Even, A. LeCorre. Appl. Surf. Sci., **258** (7), 2808 (2012).

[42] M. Niehle, J.B. Rodriguez, L. Cerutti, E. Tournié, A. Trampert. Acta Mater., **143**, 121 (2018).

[43] C.S.C. Barrett, A. Atassi, E.L. Kennon, Z. Weinrich, K. Haynes, X.-Y. Bao, P. Martin, K.S. Jones. J. Mater. Sci., **54** (9), 7028 (2019).

[44] A.C. Lin, M.M. Fejer, J.S. Harris. J. Cryst. Growth, **363**, 258 (2013).

[45] R.M. Tromp, A.W.D. van der Gon, M.C. Reute. Phys. Rev. Lett., **68** (15), 2313 (1992).

[46] J. Wasserfall, W. Ranke. Surf. Sci., **315** (3), 227 (1994).

[47] M.L. Yu, D.J. Vitkavage, B.S. Meyerson. J. Appl. Phys., **59** (12), 4032 (1986).

[48] Z. Wang, H. Guo, S. Shao, M. Saghayezhian, J. Li, R. Fittipaldi, A. Vecchione, P. Siwakoti, Y. Zhu, J. Zhang, E.W. Plummer. PNAS, **115** (38), 9485 (2018).

[49] R.L. Schwoebel. J. Appl. Phys., **40** (2), 614 (1969).

[50] Y. Horikoshi, H. Yamaguchi, F. Briones, M. Kawashima. J. Cryst. Growth, **105** (1–4), 326 (1990).

[51] Y. Li, L.J. Giling. J. Cryst. Growth, **163** (3), 203 (1996).

[52] A.C. Lin, M.M. Fejer, J.S. Harris. J. Cryst. Growth, **363**, 258 (2013).

[53] S.Y. Woo, S. Hosseini Vajargah, S. Ghanad-Tavakoli, R.N. Kleiman, G.A. Botton. J. Appl. Phys., **112** (7), 074306 (2012).